more stable in solution as five-coordinate Zn(TPP)(THF), explains why crystals of **1** function so nicely as a host lattice for the spin-labeled porphyrins.

Acknowledgment. The Nicolet R3m/E X-ray diffractometer and crystallographic computing system at Colorado State University were purchased with funds provided by the National Science Foundation (Grant CHE 81-03011). The support of NIH Grant GM21156 (G.R.E.) and NSF Grant RII-8310301 (S.S.E.) is gratefully acknowledged. C.K.S. thanks Professor Steven H. Strauss for helpful discussions.

Registry No. 1, 98689-71-5.

Supplementary Material Available: Listings of bond lengths and angles for the phenyl groups (Table VII), anisotropic thermal parameters (Table VIII), calculated hydrogen atom positions (Table IX), selected least-squares planes (Table X), and structure factors (calculated and observed; Table XI) (23 pages). Ordering information is given on any current masthead page.

Contribution from the Department of Chemistry, University of Cincinnati, Cincinnati, Ohio 45221

Chelate and Steric Effects in the Aquation of the (Thiolato)chromium(III) Complexes $[(en)_2Cr(S-X-COO)]^+$ Where X = $-CH_2-$, $-CH_2CH_2-$, and $-C(CH_3)_2-$: Anchimeric Assistance in Competitive Cr-S, Cr-N, and C-O Bond Fission[1]

I. KOFI ADZAMLI and EDWARD DEUTSCH*

Received April 5, 1985

Hydrolysis of the (thiolato)chromium(III) complexes $[(en)_2Cr(S-X-COO)]^+$, where X = $-CH_2-$, $-CH_2CH_2-$, and $-C(CH_3)_2-$, is a complicated process. The initial step of this process involves acid-catalyzed Cr-S bond cleavage, but the $[(en)_2Cr(OH_2)(OOC-X-SH)]^{2+}$ product of this step can then undergo three subsequent reactions based on the nucleophilicity of the pendant thiol moiety. (1) The pendant thiol can displace coordinated water to re-form the Cr-S linkage and regenerate the starting thiolato complex. (2) The pendant thiol can anchimerically assist C-O bond fission to eliminate the entire thiolato ligand and produce $[(en)_2Cr(OH_2)_2]^{3+}$. (3) The pendant thiol can anchimerically assist Cr-N bond fission to yield higher charged complexes that also contain pendant thiol moieties and can thus react further. The relative rates of these three subsequent reactions are dependent on the size of the ring formed upon attack by the pendant thiol. Formation of five-membered rings is favored over formation of six-membered rings. Thus, C-O bond fission is favored for X = $-CH_2CH_2-$, but Cr-S bond formation and Cr-N bond fission are favored for X = $-CH_2-$ and $-C(CH_3)_2-$. C-O bond fission is especially unfavorable when X = $-C(CH_3)_2-$, because the extra methyl groups further hinder formation of the already sterically restricted four-membered ring required for this process. Anchimerically assisted Cr-N bond fission is at least 2 orders of magnitude faster than unassisted Cr-N bond fission and is competitive with Cr-S bond fission. This leads to the observation of complicated kinetic profiles for the rupture of the Cr-S bond, which can be monitored at the characteristic ligand-to-metal charge-transfer absorption band of these complexes. Some of these complexities can be resolved by the use of initial-rate techniques for the complex with X = $-CH_2CH_2-$ and by analysis of the rate data for the complex with X = $-C(CH_3)_2-$ within a consecutive first-order reaction scheme. Comparable rate parameters governing acid-catalyzed Cr-S bond fission at 25°C with μ = 1.00 M ($HClO_4/LiClO_4$) are $(19 \pm 3) \times 10^{-4}$, $(11.1 \pm 0.2) \times 10^{-4}$, and $(8.0 \pm 0.3) \times 10^{-4}$ M^{-1} s^{-1} for X = $-CH_2CH_2-$, $-CH_2-$, and $-C(CH_3)_2-$, respectively. The significantly larger rate for the complex with X = $-CH_2CH_2-$ results at least in part from the greater basicity of the sulfur atom in the more flexible six-membered ring. At μ = 4.00 M and at 25 °C, the K_a values for the protonated complexes are estimated to be 0.35 M for X = $-CH_2CH_2-$, 1.2 M for X = $-CH_2-$, and >4 M for X = $-C(CH_3)_2-$. Overall, the rates of initial Cr-S bond fission in these complexes are remarkably similar and are not strongly influenced by the chelate and steric effects that dominate the subsequent reactions of $[(en)_2Cr(OH_2)(OOC-X-SH)]^{2+}$.

Introduction

The chemistry of coordinated sulfur and the relevance of this chemistry to biological systems have been recently reviewed in detail.[2] The chemistry of thiolato complexes is of special relevance in this area because of the prevalence of thiol-metal interactions in many metalloenzymes.[3] In order to elucidate the general reactivity patterns of thiolato ligands, we have prepared several complexes of the general formula $[(en)_2M(X)]^{n+}$, where M represents Co(III) or Cr(III) and X represents one of several bidentate-*N,S* or bidentate-*O,S* ligands. An early investigation[4] into the lability of the M-S bond showed that the Co(III) complexes $[(en)_2Co(SCH_2CH_2NH_2)]^{2+}$ and $[(en)_2Co(SCH_2COO)]^+$ are remarkably resistant to hydrolysis and acid media but that the Cr(III) analogues $[(en)_2Cr(SCH_2CH_2NH_2)]^{2+}$ and $[(en)_2Cr(SCH_2COO)]^+$ undergo rapid acid-catalyzed Cr-S bond fission, as well as acid-independent Cr-S and Cr-N bond cleavage. The chemistry of the Cr-S bond fission process is complex, and more than one hydrolysis product is observed. In order to further elucidate the chemistry and reactivity of the thiolato-chromium(III) linkage, the related complexes $[(en)_2Cr(SCH_2CH_2COO)]^+$ and $[(en)_2Cr(SC(CH_3)_2COO)]^+$ have been prepared. In this paper we report on the kinetics and mechanism of the acid-catalyzed hydrolysis of these two complexes, as well as on the nature of the products arising from hydrolysis of all three of the related complexes $[(en)_2Cr(S-X-COO)]^+$, where X = $-CH_2-$, $-CH_2CH_2-$, and $-C(CH_3)_2-$.

Experimental Section

Materials. Doubly distilled water was used in all work. Common laboratory chemicals were of reagent grade and were used without further purification. G. F. Smith doubly vacuum-distilled 70-72% perchloric acid was used in all kinetic experiments. Dowex 50W-X2, 200-400 mesh, cation-exchange resin was cleaned and converted to the lithium form before use.[5] Well-characterized, and purified, perchlorate salts of (2-mercaptoacetato-*O,S*)bis(ethylenediamine)chromium(III), (3-mercaptopropionato-*O,S*)bis(ethylenediamine)chromium(III), and (2-methyl-2-mercaptopropionato-*O,S*)bis(ethylenediamine)chromium(III) (i.e., the title complexes with X = $-CH_2-$, $-CH_2CH_2-$, and $-C(CH_3)_2-$, respectively) were available from previous studies.[4,6]

Product Analyses. Approximately 50 mg of each complex was dissolved in 25 mL of aqueous reaction medium at room temperature, and the hydrolysis reaction was allowed to proceed for various periods of time.

(1) Abstracted in part from: Adzamli, I. K. M.S. Thesis, University of Cincinnati, 1975.
(2) Deutsch, E.; Root, M. J.; Nosco, D. L. In "Advances in Inorganic and Bioinorganic Reaction Mechanisms"; Sykes, A. G., Ed.; Academic Press: London, 1982; Vol. 1, p 269.
(3) (a) Lovenberg, W. *Met. Ions Biol.* **1973**, *1*; **1973**, *2*; **1976**, *3*. (b) Timkovich, R.; Dickerson, R. E. *Enzymes (3rd Ed.)* **1976**, *11*, 347. (c) Spiro, T. G. *Met. Ions Biol.* **1982**, *4*. (d) Sigel, H. *Met. Ions Biol. Syst.* **1981**, *13*.
(4) Weschler, C. J.; Deutsch, E. *Inorg. Chem.* **1973**, *12*, 2682.
(5) Deutsch, E.; Taube, H. *Inorg. Chem.* **1968**, *7*, 1532.
(6) Adzamli, I. K.; Deutsch, E. *Inorg. Chem.* **1980**, *19*, 1366.

0020-1669/85/1324-4086$01.50/0 © 1985 American Chemical Society

The aqueous media contained various concentrations of $HClO_4$, but ionic strength was maintained at 1.0 or 4.0 M with $LiClO_4$. Reactions were quenched by 10-fold dilution with chilled water, and the product mixtures were separated on a chilled (ca. 5 °C) cation-exchange column using $NaClO_4$ (pH 3) eluants. Separations were conducted in a cold room at ca. 5 °C. The several separated fractions were collected, and each was analyzed for total chromium[5,7] and total thiol[8,9] content. Chromium was spectrophotometrically determined as chromate after alkaline peroxide oxidation (ϵ_{372} = 4820 M^{-1} cm^{-1});[5,7] each sample was analyzed in triplicate, and the average range of observed values was less than 1%. Total thiol content was spectrophotometrically determined by using 2,2'-dithiobis(pyridine), which is reduced by the thiol to 2-thiopyridone (ϵ_{343} = 8090 M^{-1} cm^{-1});[8,9] each sample was analyzed in triplicate within 2 h of its preparation, and the average range of observed values was less than 2%. Recoveries of chromium ranged from 90% to 93%, while recoveries of thiol ranged from 90% to 99%.

Kinetic Measurements and Calculations. Kinetic experiments were conducted in aqueous $HClO_4/LiClO_4$ solutions maintained at a constant ionic strength of 1.00 or 4.00 M. Reactions were monitored spectrophotometrically for at least 4 half-lives either at the 255-nm LTMCT (ligand-to-metal charge-transfer) transition characteristic of the chromium–sulfur bond[4] or at the 310-nm shoulder in the spectrum of $[(en)_2Cr(SCH_2CH_2COO)]^+$. The derived first-order rate constants were independent of the monitoring wavelength. For most of the reactions of $[(en)_2Cr(SCH_2CH_2COO)]^+$, infinite-time measurements, OD_∞, could be determined experimentally and plots of log ($OD_\infty - OD_t$) vs. time gave straight lines for at least 4 half-lives of reaction. Linear least-squares analysis yielded values of k_{obsd} and $\sigma_{k_{obsd}}$. In those instances where OD_∞ could not be determined experimentally, the Kezdy procedure[10] was employed to calculate k_{obsd} and $\sigma_{k_{obsd}}$. For reactions of $[(en)_2Cr(SC(CH_3)_2COO)]^+$ at $[H^+] > 0.40$ M (μ = 1.00 M, 25 °C) and at all $[H^+]$ (μ = 1.00 M, 5 and 15 °C), plots of log ($OD_\infty - OD_t$) vs. time were linear for over 4 half-lives of reaction. However, at $[H^+] < 0.40$ M (μ = 1.00 M, 25 °C) and at all $[H^+]$ (μ = 1.00 M, 35 and 45 °C) these plots were not linear but rather were indicative of the presence of two consecutive first-order reactions. The OD_t–t data for these reactions were fitted to the expression

$$OD_t - OD_\infty = A \exp(-k_{fast}t) + B \exp(-k_{slow}t) \quad (1)$$

by using a previously described nonlinear least-squares procedure.[11] The hydrolyses of both $[(en)_2Cr(SCH_2CH_2COO)]^+$ and $[(en)_2Cr(SC(CH_3)_2COO)]^+$ were also monitored by using an initial-rate technique wherein less than the initial 10% of reaction was considered. Activation parameters were calculated within the Eyring formalism by linear least-squares analyses of ln (k/T) vs. $1/T$ plots. Each value of k_{obsd} was weighted as $(1/\sigma_{k_{obsd}})^2$. All reported errors are standard deviations.

Results

The three complexes investigated herein have been previously characterized.[4,6] Of chief interest to this study is the fact that the electronic spectra of all three complexes exhibit a distinctive ligand-to-metal charge-transfer (LTMCT) absorption at ca. 255 nm, which is characteristic of the Cr–S linkage. This absorption disappears upon hydrolysis of the Cr–S bond.

Product Analyses. Hydrolysis of each complex leads to three products, which are characterized by charge (as determined by ion-exchange elution characteristics), total thiol content, and total chromium content (Table I). The distribution of these products as a function of time, $[H^+]$, and ionic strength are summarized in Table A.[12] At short reaction times only the +1-charged starting material and a +2-charged, orange product (band I) are observed. This +2 product does not exhibit the LTMCT band characteristic of the Cr–S linkage and contains a Cr/S ratio of 1.0 (Table I). It is therefore assigned to be the aquation product resulting from initial Cr–S bond fission, i.e. $[(en)_2Cr(OH_2)(OOC-X-SH)]^{2+}$. When X = $-CH_2-$ or $-C(CH_3)_2-$, raising the pH of the reaction medium induces re-formation of the Cr–S bond, but when X = $-CH_2CH_2-$, no such Cr–S bond re-formation is observed.

Table I. Analysis of Products Resulting from the Aquation of $[(en)_2Cr(S-X-COO)]^+$ Complexes[a]

	product band[b]	% Cr	% thiol
X = $-CH_2CH_2-$	0	0	60
	I	33	38
	II	58	2
	III	9	0
X = $-CH_2-$	0	0.6	62
	I	30	29
	II	49	6
	III	20	4
X = $-C(CH_3)_2-$	0	1	25
	I	62	59
	II	26	12
	III	10	4

[a] Conditions: 25 °C, μ = $[H^+]$ = 4.0 M; time of reaction >4 half-lives. Reported percentages are based on the total amount of recovered product: % Cr = percentage of recovered chromium in indicated band; % thiol = percentage of recovered thiol in indicated band. [b] Bands are identified as follows: Band 0 is the material that has no affinity for the ion-exchange column and contains all the noncoordinated thiol. Band I consists of the +2-charged, orange, product $[(en)_2Cr(OOC-X-SH)]^{2+}$. Band II contains predominantly +3-charged complexes, and has a blue-gray color. Band III contains predominantly +4-charged, or higher charged, complexes and has a gray color.

At longer reaction times, +3- (band II) and possibly +4-charged (band III) products are observed in addition to the +2 species. These higher charged products are not well separated by the chromatographic procedure, and none of them exhibits a Cr–S LTMCT band. The +3 product contains a small, but definitely detectable, amount of thiol in all three cases (Table I). The +4 product does not contain sulfur when X = $-CH_2CH_2-$ but does contain a small amount of sulfur when X = $-CH_2-$ or $-C(CH_3)_2-$ (Table I). The expected thiol-containing +3 product is $[(en)Cr(NH_2CH_2CH_2NH_3)(OH_2)_2(OOC-X-SH)]^{3+}$, while the expected +3 product not containing thiol is $[(en)_2Cr(OH_2)_2]^{3+}$. Previous ion-exchange studies[12-17] indicate that the +3 complex containing the monodentate ethylenediamine ligand should be eluted before $[(en)_2Cr(OH_2)_2]^{3+}$. The +4 product is assigned to be a mixture of $[(en)Cr(NH_2CH_2CH_2NH_3)(OH_2)_3]^{4+}$ and $[Cr(NH_2CH_2CH_2NH_3)_2(OH_2)_3(OCC-X-SH)]^{4+}$.

Kinetics. (i) $[(en)_2Cr(SCH_2CH_2COO)]^+$. Observed first-order rate constants for the hydrolysis of this complex are compiled in Table B.[12] Plots of k_{obsd} vs. $[H^+]$ are curved with zero intercepts, while plots of $1/k_{obsd}$ vs. $1/[H^+]$ are linear. Thus the acid dependence of k_{obsd} is adequately described by

$$k_{obsd} = bK[H^+]/(1 + K[H^+]) \quad (2)$$

with $b = 3.5 \times 10^{-3}$ s^{-1} and K = 0.5 M^{-1} at 25 °C and μ = 1.00 M. However, the results of the product analyses (Tables I and A[12]) clearly show that Cr–N bond fission is competitive with this Cr–S bond fission monitored at 255 or 310 nm. Experiments in the visible region, where Cr–N bond fission dominates the spectral changes,[4] confirm this conclusion. The Cr–S bond fission process can be isolated by the use of the initial-rate technique, and the results of these experiments are given in Table C.[12] The acid dependence of k_{obsd} is again described by eq 2, and in fact the initial-rate data fit eq 2 better than do the composite-rate data. In all cases the k_{obsd} value determined from initial-rate data is less than, or equal to, that rate determined from composite-rate data, and the difference increases with increasing $[H^+]$. This relationship is apparent from the summary of k_{obsd} data given in Table II. Nonlinear least-squares analysis of the initial-rate data

(7) Haupt, G. W. *J. Res. Natl. Bur. Stand. (U.S.)* **1952**, *48*, 414.
(8) Lavallee, D. K.; Sullivan, J. C.; Deutsch E. *Inorg. Chem.* **1973**, *12*, 1440.
(9) Grassetti, D. R.; Murray, J. F., Jr. *Arch. Biochem. Biophys.* **1967**, *119*, 41.
(10) Kezdy, F. J.; Jaz, J.; Bruylants, A. *Bull. Soc. Chim. Belg.* **1958**, *67*, 687.
(11) Moore, R. H.; Ziegler, R. K. Report No. LA-2367 plus Addenda; Los Alamos Scientific Laboratory: Los Alamos, NM, 1959.
(12) Supplementary material. This includes all tables designated by alphabetic characters.
(13) Linck, R. G. *Inorg. Chem.* **1977**, *16*, 3143.
(14) Bifano, C.; Linck, R. G. *Inorg. Chem.* **1974**, *13*, 609.
(15) Childers, R. F., Jr.; van der Zyl, K. G., Jr.; House, D. A.; Hughes, R. G.; Garner, C. S. *Inorg. Chem.* **1968**, *7*, 749.
(16) Viegel, J. M.; Garner, C. S. *Inorg. Chem.* **1965**, *4*, 1569.
(17) Pyke, S. C.; Linck, R. G. *Inorg. Chem.* **1971**, *10*, 2445.
(18) Espenson, J. H.; Carlyle, D. W. *Inorg. Chem.* **1966**, *5*, 586.

Table II. Observed Rate Constants Governing Aquation of $[(en)_2Cr(S-X-COO)]^+$ Complexes[a]

	10^4k_{obsd}, s^{-1}			
$[H^+]$, M	X = $-CH_2-$[b]	X = $-CH_2CH_2-$[c]	X = $-CH_2CH_2-$[d]	X = $-C(CH_3)_2-$[e]
0.088	1.15 ± 0.01			
0.100		1.46 ± 0.06	1.34 ± 0.09	1.29 ± 0.04
0.114		1.67 ± 0.06		
0.113		1.95 ± 0.07	2.5 ± 0.1	
0.200	2.54 ± 0.01	2.93 ± 0.09		2.8 ± 0.3
0.330	3.89 ± 0.03			3.32 ± 0.04
0.400		5.8 ± 0.1	5.1 ± 0.1	3.85 ± 0.03
0.500		6.8 ± 0.1		4.43 ± 0.01
0.600	7.39 ± 0.02	7.7 ± 0.1		5.44 ± 0.02
0.700				6.22 ± 0.01
0.800	9.61 ± 0.03	9.7 ± 0.1		6.78 ± 0.05
0.900			7.9 ± 0.2	7.45 ± 0.04
1.00	11.2 ± 0.1	10.8 ± 0.2		

[a] Conditions: 25 °C, μ = 1.00 M. [b] Data from ref 4. [c] Composite-rate data. [d] Initial-rate data. [e] Both k_{obsd} and k_{fast} values.

gives the following parameters for Cr–S bond fission uncomplicated by competitive Cr–N bond cleavage (25 °C, μ = 1.00 M): $b = (1.7 \pm 0.2) \times 10^{-3}$ s^{-1}; $K = (1.1 \pm 0.2)$ M^{-1}. Activation and thermodynamic parameters, estimated by linear least-squares analysis of data spanning only a 10 °C temperature range, are as follows: $\Delta H_b^* = 12$ kcal/mol; $\Delta H_K^\circ = -9$ kcal/mol; $\Delta S_b^* = -12$ eu; $\Delta S_K^\circ = -31$ eu.

(ii) $[(en)_2Cr(SC(CH_3)_2COO)]^+$. Both the rate law and rate-governing hydrolysis of this complex are dependent on $[H^+]$ and temperature. These dependences, assessed at μ = 1.00 M, are summarized as follows:

(a) At 5 and 15 °C, the hydrolysis is first order for more than 95% of the reaction and k_{obsd} is linearly dependent on $[H^+]$. Values of k_{obsd} are given in Table D.[12]

(b) At 25 °C and $[H^+] > 0.40$ M, the hydrolysis is still first order and k_{obsd} still varies linearly with $[H^+]$. But at $[H^+] < 0.40$ M, the hydrolysis is no longer simply first order but rather occurs by two consecutive first-order reactions. Nonlinear least-squares analysis[11] of the OD_t–t data within eq 1 yields values of k_{fast} that satisfy the same linear k_{obsd}–$[H^+]$ relationship as do the k_{obsd} values resulting from experiments at $[H^+] > 0.40$ M. These values of k_{fast} are also incorporated into Table D.[12]

(c) The linear dependence of k_{obsd} (and k_{fast}) on $[H^+]$ at 5, 15, and 25° C can be summarized by the following expression and parameters:

$$k_{obsd} = c + d[H^+] \quad (3)$$

$c(25\ °C) = (0.54 \pm 0.16) \times 10^{-4}$ s^{-1}; $d(25\ °C) = (8.0 \pm 0.3) \times 10^{-4}$ M^{-1} s^{-1}. The c term does apparently represent a real acid-independent path, but the temperature dependence of this term is not sufficiently defined by the existing data to allow calculation of activation parameters. Activation parameters, estimated by linear least-squares analysis, for the d term are $\Delta H_d^* = 21.4 \pm 0.4$ kcal/mol and $\Delta S_d^* = -0.7 \pm 1.4$ eu.

(d) At 35 and 45 °C the hydrolysis occurs by two consecutive first-order reactions at all $[H^+]$ values investigated. Nonlinear least-squares analysis[11] within eq 1 yields values of k_{fast} that are again linearly dependent on $[H^+]$, but the errors associated with the derived parameters are too large to permit further analysis of these data. These k_{fast} data, as well as k_{slow} parameters from all analyses, are listed in Table E.[12]

When the ionic strength is raised from 1.0 to 4.0 M at 25 °C, the rate law for hydrolysis at $[H^+] > 0.40$ M changes from simple first order to consecutive first order. Nonlinear least-squares analysis of these data within eq 1 leads to the values of k_{fast} that are given in Table D.[12] The $[H^+]$ dependence of these derived values of k_{fast} are adequately described by eq 3 with $c = (4.1 \pm 0.3) \times 10^{-3}$ s^{-1} and $d = (1.08 \pm 0.12) \times 10^{-3}$ M^{-1} s^{-1}.

The results of initial-rate experiments at both μ = 1.00 M (25 and 35 °C) and μ = 4.00 M (25 °C) are given in Table F.[12] Rate constants determined by this technique have unusually large associated errors ($\sigma_{k_{obsd}}$), indicating that Cr–N bond fission competes with Cr–S bond fission even at very early reaction times. At μ = 4.00 M the dependence of k_{obsd} on $[H^+]$ is adequately

Scheme I

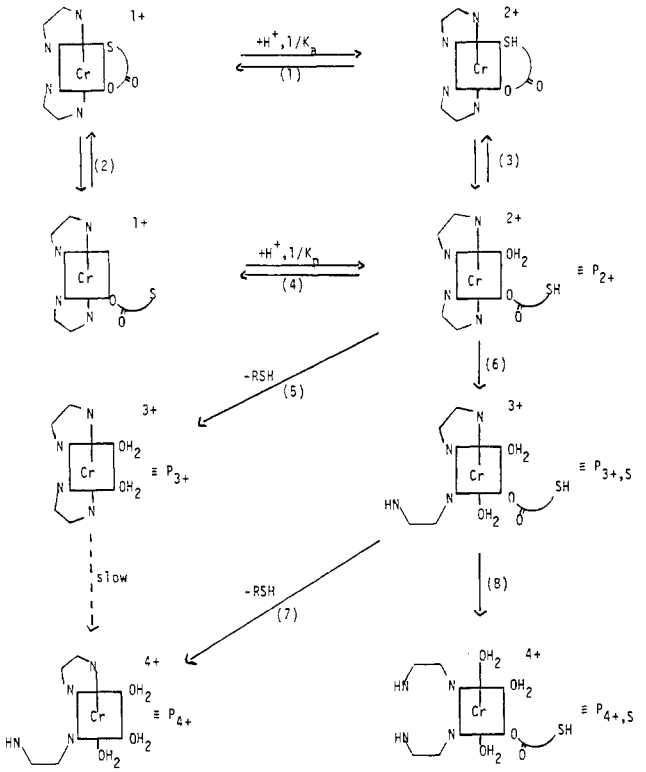

expressed by eq 3 with $c = (2.9 \pm 0.4) \times 10^{-3}$ s^{-1} and $d = (6.4 \pm 1.4) \times 10^{-4}$ M^{-1} s^{-1}. However, at μ = 1.00 M the intercept term is not statistically significant and $k_{obsd} = d[H^+]$: $d(25\ °C) = (6.6 \pm 0.6) \times 10^{-4}$ M^{-1} s^{-1} and $d(35\ °C) = (23 \pm 2) \times 10^{-4}$ M^{-1} s^{-1}.

Discussion

The following abbreviations are used in this section:

$$Cr(tga) \equiv [(en)_2Cr(SCH_2COO)]^+$$

$$Cr(tpa) \equiv [(en)_2Cr(SCH_2CH_2COO)]^+$$

$$Cr(tiba) \equiv [(en)_2Cr(SC(CH_3)_2COO)]^+$$

These three complexes are also represented as $[(en)_2Cr(S-X-COO)]^+$ with X = $-CH_2-$, $-CH_2CH_2-$, and $-C(CH_3)_2-$.

All of the stoichiometric and kinetic results obtained in this study, as well as the kinetic results obtained earlier with Cr(tga),[4] can be accounted for by the general mechanism presented in Scheme I. Steps 1–4 of this scheme are just those that have been proposed previously to account for the acid-catalyzed aquation of Cr(tga).[4] Steps 5–7 have been added to account for the results of the product analyses presented herein and also to account for the more complicated kinetics observed for the hydrolysis of Cr(tpa) and Cr(tiba).

Anchimeric Assistance. Anchimeric assistance by thiol and thioether groups is well established in the organic chemistry of sulfur compounds. Fuson et al.[19] postulate three-membered cyclic sulfonium intermediates in nucleophilic displacement reactions such as

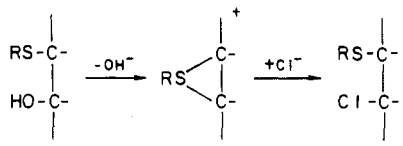

(4)

and the same three-membered sulfonium intermediate is theorized[20] to be responsible for the stereospecificity of RSCl addition to olefins. Similarly, five-membered and six-membered cyclic sulfonium intermediates have been proposed in the reaction of ethoxide with 4-bromo and 5-bromo sulfides.[21] Thus, a pendant sulfur-containing moiety can anchimerically assist nucleophilic displacement reactions by forming three-membered to six-membered rings, despite the ring strain inherent in these structures.

Product Analyses. Scheme I depicts the several products for which evidence has been obtained in these studies. The initial +2-charged product, designated in Scheme I as P_{2+}, arises from Cr–S bond fission and is the major product obtained at short reaction times. P_{2+} elutes from ion-exchange columns as a single band, which is designated band I in Tables I and A.[12]

The initial hydrolysis product P_{2+} can undergo three subsequent reactions. (1) By path 3 it can re-form the Cr–S bond and regenerate the starting thiolato complex. (2) By path 5 the pendant thiol moiety can achimerically assist C–O (or Cr–O) bond fission to eliminate the entire thiolato ligand and produce $[(en)_2Cr(OH_2)_2]^{3+}$ (P_{3+}). Path 5 accounts for the fact that the thiol content of band 0 (i.e., the material that passes through the cation-exchange column without retention) is approximately equal to the chromium content of band III. Thus, band 0 consists predominantly of noncoordinated thiol, and band III consists predominantly of P_{3+}, $[(en)_2Cr(OH_2)_2]^{3+}$. (3) The small but finite amount of thiol in band III indicates that the pendant thiol moiety of P_{2+} can also anchimerically assist Cr–N bond fission to yield $P_{3+,S}$ via path 6. Since $P_{3+,S}$ carries a net +3 charge, it coelutes with P_{3+} in band III.

The pendant thiol moeity of $P_{3+,S}$ is still capable of anchimerically assisting C–O (or Cr–O) bond fission to yield the +4-charged product P_{4+} plus noncoordinated thiol via path 7. It can also assist Cr–N bond fission to yield a +4-charged product that contains thiol, i.e. $P_{4+,S}$.

The salient feature of Scheme I is the ability of the pendant thiol moiety to function as a nucleophile and (a) displace coordinated water by path 3, (b) anchimerically assist C–O (or Cr–O) bond fission by paths 5 and 7, and (c) anchimerically assist Cr–N bond fission by paths 6 and 8. The relative rates of these reactions are dependent on the size of the ring formed upon attack by the pendant thiol. For those reactions in which the pendant thiol moiety attacks a ligand situated cis to the carboxylate group (i.e., paths 3, 6, and 8), the rate is faster for the complexes forming five-membered rings (i.e., Cr(tga) and Cr(tiba)). The extra $-CH_2-$ linkage in Cr(tpa) places the pendant thiol moiety one atom further from the chromium center, and this apparently decreases significantly its ability to function as an internal nucleophile. This relative inefficiency of forming a six-membered ring, relative to forming a five-membered ring, is manifested in three experimental observations. (i) The re-formation of the Cr–S bond (path 3) proceeds readily at low $[H^+]$ for the five-membered chelate compounds Cr(tga)[4] and Cr(tiba) but does not proceed detectably for the six-membered chelate compound Cr(tpa). (ii) The relative efficiency of thiol-induced Cr–N bond fission in forming the +3-charged products is given by $k_6/(k_5 + k_6)$, which is just the ratio of % thiol in band II to % Cr in band II (band II is comprised of two +3-charged products: P_{3+}, which does not contain a thiol, and $P_{3+,S}$, which does). For Cr(tpa) this ratio is only 0.04, while for Cr(tga) and Cr(tiba) it is 0.12 and 0.45, respectively (Table I). (iii) Similarly, the relative efficiency of thiol-induced Cr–N bond fission in forming the +4-charged products is given by the ratio of % thiol to % Cr in band III. For Cr(tpa) this ratio is 0, while for Cr(tga) and Cr(tiba) it is 0.18 and 0.37, respectively (Table I).

Attack of the pendant thiol moiety on the coordinated carboxylate group (paths 5 and 7) is favored for the complex containing the six-membered ring (i.e., Cr(tpa)). The relative efficacy of this mode of anchimeric assistance in forming the +3-charged products is given by $k_5/(k_5 + k_6)$, which is 0.96 for Cr(tpa) vs. 0.88 and 0.55 for Cr(tga) and Cr(tiba), respectively (Table I). The corresponding values for the +4-charged products are 1.00 for Cr(tpa) vs. 0.82 and 0.63 for Cr(tga) and Cr(tiba), respectively. In this reaction the extra $-CH_2-$ linkage of Cr(tpa) is an advantage, implying that the pendant sulfur atom attacks the C–O linkage (five-membered ring) rather than the Cr–O linkage (six-membered ring). For Cr(tga) and Cr(tiba), attack at the C–O linkage involves formation of a relatively unfavorable four-membered ring, and the extra methyl groups of Cr(tiba) apparently further hinder formation of this sterically restricted four-membered ring.

It should be noted that the rate of thiol-induced Cr–N bond fission observed in this study ($k \simeq 10^{-4}$ s^{-1}) is at least 2 orders of magnitude greater than the rate of unassisted Cr–N bond fission in ammine- and ethylenediamine-chromium(III) complexes ($k \simeq 10^{-8}$–10^{-6} s^{-1} [14]). This anchimerically assisted bond cleavage by a cis-situated ligand is analogous to the "cartwheel" mechanism proposed for carbonate and nitrate labilization of complexes[22,23] and is similar to the internal conjugate-base mechanism proposed by Rorabacher[24] and promulgated by Margerum.[25,26]

Kinetics. Scheme I accounts for the complicated kinetics observed in this study. Since the hydrolysis reaction is monitored at the ligand-to-metal charge-transfer band resulting from the Cr–S linkage, the observed decrease in absorbance reflects cleavage of this bond. Paths 3 and 6, both of which are reversible, effect the formation and breaking of the Cr–S bond. Path 6 occurs after path 3 and also incorporates the energetics of Cr–N bond fission. Thus, in general, the kinetics of Cr–S bond fission should follow a consecutive reaction profile, but this can degenerate to a first-order profile if the two rates are vastly different or approximately equal.[27] With use of initial-rate techniques, path 3 may possibly be isolated from the effects of path 6. Under these conditions Scheme I reduces to Scheme II, which has been previously discussed in detail.[4]

Scheme II

$$H^+ + (en)_2Cr(S\text{–}X\text{–}COO)^+ \overset{1/K_a}{\rightleftharpoons} [(en)_2Cr(S\text{–}X\text{–}COO)H]^{2+}$$

$$(en)_2Cr(S\text{–}X\text{–}COO)^+ + H_2O \overset{k_0}{\underset{k_{-0}}{\rightleftharpoons}} (en)_2Cr(OH_2)(OCC\text{–}X\text{–}S)^+$$

$$[(en)_2Cr(S\text{–}X\text{–}COO)H]^{2+} + H_2O \overset{k_1}{\underset{k_{-1}}{\rightleftharpoons}} (en)_2Cr(OH_2)(OOC\text{–}X\text{–}SH)^{2+}$$

$$(en)_2Cr(OH_2)(OOC\text{–}X\text{–}S)^+ + H^+ \overset{1/K_p}{\rightleftharpoons} (en)_2Cr(OH_2)(OOC\text{–}X\text{–}SH)^{2+}$$

Scheme II leads to the following rate law governing reaction in the forward direction

(19) Fuson, R. C.; Price, C. C.; Burness, D. M. *J. Org. Chem.* **1946**, *11*, 475.
(20) Mueller, W. H. *Angew. Chem., Int. Ed. Engl.* **1969**, *8*, 482.
(21) Knipe, A. C.; Stirhng, C. J. M. *J. Chem. Soc. B* **1968**, 1218.
(22) Swaddle, T. W.; Guastalla, G. *Can. J. Chem.* **1974**, *52*, 527.
(23) Guastalla, G.; Swaddle, T. W. *Inorg. Chem.* **1974**, *13*, 61.
(24) Rorabacher, D. B. *Inorg. Chem.* **1966**, *5*, 1891.
(25) Read, R. A.; Margerum, D. W. *Inorg. Chem.* **1981**, *20*, 3143.
(26) Margerum, D. W. In "Mechanistic Aspects of Inorganic Reactions"; American Chemical Society: Washington, DC, 1982; ACS Symp. Ser. No. 198, p 3.
(27) Buckingham, D. A.; Francis, D. J.; Sargeson, A. M. *Inorg. Chem.* **1974**, *13*, 2630.

$$k_{obsd} = \frac{k_0 + k_1[H^+]/K_a}{1 + [H^+]/K_a} \quad (5)$$

which reduces to

$$k_{obsd} = \frac{k_1[H^+]/K_a}{1 + [H^+]/K_a} \quad (5a)$$

when k_0 is very small. This is equivalent to the experimentally observed rate law given in eq 2, with $b = k_1$ and $K = 1/K_a$.

(i) Cr(tpa). Even though the individual hydrolysis reactions appear to be first order and the resulting k_{obsd} values are adequately described by eq 2, it is clear that for this complex the rates of Cr–S and Cr–N bond fission are competitive. The k_{obsd} values obtained from initial-rate experiments reflect only Cr–S bond fission and consequently fit eq 2 better than do the composite k_{obsd} values.

(ii) Cr(tiba). The hydrolysis reactions of this complex exhibit the biphasic rate profile expected from the consecutive operation of paths 3 and 6 in Scheme I. The faster component can be made dominant by lowering the reaction temperature, implying that the slower component has a higher activation energy. This is consistent with the fast component reflecting pure Cr–S bond fission (path 3) and the slow component incorporating Cr–N bond fission (path 6), since ΔH^* values for Cr–N bond fission are significantly greater than those for Cr–S bond fission (ca. 25 kcal/mol[12-17] vs. ca. 10 kcal/mol[4]). The $[H^+]$ dependence of the k_{obsd} values governing the faster component is expressed by eq 3 rather than eq 2. In the context of Scheme II and eq 5, this corresponds to the rate law

$$k_{obsd} = k_0 + k_1[H^+]/K_a \quad (5b)$$

with $[H^+]/K_a \ll 1$, $c = k_0$, and $d = k_1/K_a$.

Some typical rate data governing hydrolysis of the three $[(en)_2Cr(S-X-COO)]^+$ complexes are given in Table II. The similarity of the observed rates of these three processes is quite remarkable, there being generally less than a 30% variation at any given $[H^+]$. Since the net hydrolysis reaction is so complicated, the only rate parameter that can be confidently extracted from the observed data is that governing acid-catalyzed Cr–S bond fission, i.e. k_1/K_a in Scheme II. From initial-rate data for Cr(tpa), k_{obsd} data for Cr(tga), and k_{obsd} plus k_{fast} data for Cr(tiba), values of $10^4k_1/K_a$ (25 °C, μ = 1.00 M) for Cr(tpa), Cr(tga), and Cr(tiba) are 19 ± 3, 11.1 ± 0.2, and 8.0 ± 0.3 M^{-1} s^{-1}, respectively. The significantly larger value of k_1/K_a for Cr(tpa) arises at least in part from the fact that K_a for the protonated form of this complex is significantly smaller than those for the protonated forms of the other two. At μ = 1.00 M, Cr(tpa) is sufficiently basic that plots of k_{obsd} vs. $[H^+]$ curve due to protonation of the coordinated sulfur atom; contrariwise, for Cr(tga) and Cr(tiba), plots of k_{obsd} vs. $[H^+]$ are linear. Thus, at μ = 1.00 M (25 °C) K_a for $Cr(tpa)H^+$ is 0.9 ± 0.2 M, while K_a values for $Cr(tga)H^+$ and $Cr(tiba)H^+$ are both estimated to be >4 M. At μ = 4.00 M (25 °C), the corresponding estimates for K_a are 0.35 M for $Cr(tpa)H^+$, 1.2 M for $Cr(tga)H^{4+}$, and >4 M for $Cr(tiba)H^+$. As expected, protonation of the positively charged complexes is more easily affected in the medium of higher ionic strength.[4,28] The greater basicity of Cr(tpa) can be explained by the greater flexibility of the six-membered chelate ring, which more readily relieves the stress engendered on converting the two-coordinate, unprotonated, sulfur atom to a three-coordinate, protonated, sulfur atom. Similarly, the chelate ring of Cr(tiba) is least flexible because of the $-C(CH_3)_2-$ linkage, and this complex has the least affinity for protons (largest K_a value for $Cr(tiba)H^+$). Concomitantly, the $10^4k_1/K_a$ value for Cr(tiba) is the smallest of the three, although the difference between the values for Cr(tiba) and Cr(tga) (8.0 ± 0.3 vs. 11.1 ± 0.2 M^{-1} s^{-1}) is too small to allow interpretation of its mechanistic significance.

The kinetic effects of chelate ring size, and steric hindrance in the chelate ring, have been the subject of several investigations.[26,29-33] In some cases steric bulk in the chelate ring increases the rate of ring opening,[33] while in others it dramatically inhibits the rate of ring opening.[26] As noted above, the difference in rates of acid-catalyzed Cr–S bond fission in Cr(tga) and Cr(tiba) is very small, indicating that in this system steric effects are not dominant. The rate of acid-catalyzed Cr–S bond fission in the title complexes appears to be dominated by the basicity of the coordinated thiolato sulfur atom and the inherent lability of the Cr–S linkage.

Acknowledgment. Financial support by the National Science Foundation (Grant No. CHE79-26497) is gratefully acknowledged.

Registry No. $[(en)_2Cr(SCH_2COO)]ClO_4$, 26743-67-9; $[(en)_2Cr(SCH_2CH_2COO)]ClO_4$, 51911-43-4; $[(en)_2Cr(SC(CH_3)_2COO)]ClO_4$, 60195-76-8.

Supplementary Material Available: Tables A–F, giving product distribution data and observed first-order rate constants (7 pages). Ordering information is given on any current masthead page.

(28) Adzamli, I. K.; Nosco, D. L.; Deutsch, E. *J. Inorg. Nucl. Chem.* **1980**, *42*, 1364.
(29) Carter, M. J.; Beattie, J. K. *Inorg. Chem.* **1970**, *9*, 1233.
(30) Mureinik, R. J. *Rev. Inorg. Chem.* **1979**, *1*, 1.
(31) Albertin, G.; Bordignon, E.; Orio, A. A.; Pavoni, B.; Gray, H. B. *Inorg. Chem.* **1979**, *18*, 1451.
(32) Kustin, K.; Swinehart, J. *Prog. Inorg. Chem.* **1970**, *13*, 148.
(33) Knebel, W. J.; Angelici, R. J. *Inorg. Chem.* **1974**, *13*, 627, 632.